

S. Aisayev*, U. Zhabasbayev*, K. Turegeldiyeva*

LAW OF DEVELOPMENT TURBULENT NON-ISOTHERMAL JET FLOW IN PIT OIL

1. INTRODUCTION

Increasing requirements for environmental protection challenge the oil industry to minimize the oil spill accidents throughout the production and transportation processes. These accidents can result in oil wastes in the form of oil pits. In this paper results of development of turbulent non-isothermal round jet flow in oil pits are provided. The turbulent jet and pit oil hydrodynamic interaction is in qualitative agreement with the data of industrial tests.

The physical model. Pit oil is a valuable hydrocarbon source, though it has been changed structurally to some extent. The thermomechanical method of oil dilution using a mobile unit was proposed for gathering packed high-paraffin condensated pit oil (Yershin *et al.*, 2002). Field tests carried out on the Zhetybai (July – August, 1994), Uzen (February, 1997), Zhalgyz Tobe (December, 2003) fields demonstrated the efficiency of the proposed method of recovering pit oil. Entering thick oil medium a supersonic steam jet flow is sharply slowed, transferring its impulse and energy to the oil mass. As a result due to the ejection property of the turbulent flow a virtually heated oil flow is formed. Thus, the interaction of a supersonic steam jet with pit oil can be considered as an injection of a non-isothermal oil jet in a limited volume.

In this case it can be assumed that a round fluid flow with an initial temperature T_o , speed U_o and flow rate G_o is injected in a high viscosity medium (oil pit). This jet velocity is subsonic, the temperature is high ($T_o = 373$ K) which allows to heat the high viscosity medium. It is assumed that the fluid jet has the same physical and chemical properties as pit oil has and its rheological properties satisfy the Newtonian fluid model. The temperature of pit oil ($T_w = 303$ K) is just above its freezing temperature. Thus fusion heat can be ignored. As the jet progresses in the tank, its velocity goes down, the heat brought in by the hot jet heats the surrounding highly viscous medium and decrease its viscosity, hence involving pit oil in

* Kazakh-British Technical University, Kazakhstan Almaty; U.Zhabasbayev@kbtu.kz

motion. Thermophysical properties of pit oil are considered as functions of temperature and are identified in laboratory studies and with the use of reference books. They are summarized by the following empirical equations:

$$\rho = 18.5 * \exp\left(-\frac{T - T_o}{72}\right) + 821.5 \text{ (kg/m}^3)$$

$$\mu = 5.511 * \exp(-0.1487 * T) + 0.005853 \text{ (kg/(m*s))}$$

$$\lambda = 0.042 * \exp(-0.006695 * T) + 0.124 \text{ (W/(m}^0\text{C})$$
(1)

The flow diagram and integration domain are shown in Figure 1. It is assumed that pit oil is located in a cylindrical tank. The bottom and walls of a tank are hard surfaces, and the top part is a free area bordering with atmosphere air. The round hot fluid jet flow is injected in the center of a tank and its motion is analyzed in a cylindrical system of axes. The OZ axis is directed along the flow movement axis and the OR axis – along the round jet radius. The area ranging between $0 \leq z \leq L; 0 \leq r \leq R_w$ on the OZ axis is considered due to axial symmetry of the task (Fig. 1).

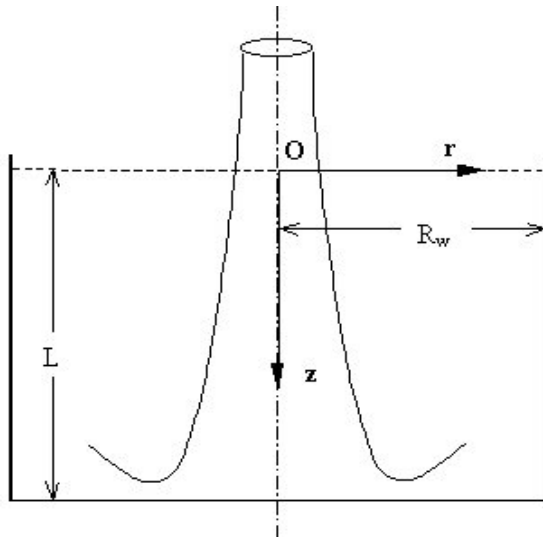


Fig. 1. Diagram of pit oil flow development

Due to high ejection properties of the jet the initial mass, initiating jet motion is much smaller than the mass of the main portion of the flow, moreover it is negligibly small compared to the mass of oil in the oil pit. This allows to ignore the increase of oil volume in an oil pit resulting from a fluid flow volume addition.

The flow motion is considered turbulent, and the process of heating pit oil regular, i.e. the amount of heat entering the oil pit equals the heat going out through the limiting surfaces.

The mathematical model of the process. The non-isothermal fluid flow motion in pit oil is described by Navier-Stokes equations, averaged by Reynolds (Abramovich *et al.*, 1960, Shlikhting *et al.*, 1974, Loytsanski *et al.*, 1987, Sebesi *et al.*, 1987) as follows

$$\rho u \frac{\partial u}{\partial z} + \rho v \frac{\partial u}{\partial r} = -\frac{\partial p}{\partial z} + 2 \frac{\partial}{\partial z} \left(\mu_\epsilon \frac{\partial u}{\partial z} \right) - \frac{2}{3} \frac{\partial}{\partial z} \left(\mu_\epsilon \operatorname{div} \vec{V} \right) + \frac{1}{r} \frac{\partial}{\partial r} \left[\mu_\epsilon r \left(\frac{\partial u}{\partial r} + \frac{\partial v}{\partial z} \right) \right] \quad (2)$$

$$\rho u \frac{\partial v}{\partial z} + \rho v \frac{\partial v}{\partial r} = -\frac{\partial p}{\partial r} + \frac{2}{r} \frac{\partial}{\partial r} \left(\mu_\epsilon r \frac{\partial v}{\partial r} \right) - \frac{2}{3} \frac{\partial}{\partial r} \left(\mu_\epsilon \operatorname{div} \vec{V} \right) + \frac{\partial}{\partial z} \left[\mu_\epsilon \left(\frac{\partial u}{\partial r} + \frac{\partial v}{\partial z} \right) \right] - \frac{2v}{r^2} \mu_\epsilon \quad (3)$$

$$\frac{\partial \rho u}{\partial z} + \frac{1}{r} \frac{\partial (\rho v r)}{\partial r} = 0 \quad (4)$$

The heat transfer equation, taking into account the dissipation of mechanical energy motion can be written as:

$$\rho c \left(u \frac{\partial T}{\partial z} + v \frac{\partial T}{\partial r} \right) = \frac{\partial}{\partial z} \left(\lambda_\epsilon \frac{\partial T}{\partial z} \right) + \frac{1}{r} \frac{\partial}{\partial r} \left(r \lambda_\epsilon \frac{\partial T}{\partial r} \right) + \Phi \quad (5)$$

where $\Phi = 2\mu_\epsilon \left[\left(\frac{\partial v}{\partial r} \right)^2 + \left(\frac{v}{r} \right)^2 + \left(\frac{\partial u}{\partial z} \right)^2 \right] + \mu_\epsilon \left(\frac{\partial u}{\partial r} + \frac{\partial v}{\partial z} \right)^2$ – dissipation of the kinetic energy motion into heat.

In equations (2)–(5): z, r – cylindrical coordinates; u, v – components of velocity vector \vec{V} ; p, ρ, T, c – pressure, density, temperature and fluid heat capacity, $\mu_\epsilon = \mu + \mu_t$, μ – dynamic viscosity of the fluid, μ_t – turbulent eddy viscosity, $\lambda_\epsilon = \lambda + \lambda_t$, λ – thermal conductivity of the fluid, $\lambda_t = c_p \mu_t / \operatorname{Pr}_t$, where Pr_t – turbulent analog of Prandtl number.

Fluid heat capacity (c) in temperature range $303 \text{ K} \leq T \leq 373 \text{ K}$ varies to a small extent and remains constant $c = 0.23 \text{ kJ} / (\text{kg} * \text{deg})$.

It is known that $(k - \epsilon)$ – turbulence model is widely used in engineering, which provides fairly reliable data (Moulden *et al.*, 1980, Koolman *et al.*, 1984, Shets *et al.*, 1984, Chen *et al.*, 1988, Menter *et al.*, 1993, Craft *et al.*, 2003, Chien *et al.*, 1982, He *et al.*, 2002). For example, Craft *et al.* (2003, pp 813–820) present the comparison results with calculations of wall-adjacent turbulent flat flow, leaking on the counter-current flow of fluid obtained from three models of turbulence: 1) most recent LES-model of turbulence, 2) $(k - \epsilon)$ – turbulence model for low Reynolds numbers, Re; 3) models of turbulent stresses using the boundary conditions of the wall law. The calculated results show that the data obtained from $(k - \epsilon)$ – turbulence model at relatively low Reynolds numbers (Re), are in good quantitative agreement with the LES-turbulence model data and experimental results (He, Xu, and Jackson, 2002, pp 487–496).

The turbulent dynamic viscosity μ_t is calculated using the $(k - \varepsilon)$ turbulence model, designed for low Reynolds numbers Re , and is given by (Chien *et al.*, 1982):

$$\mu_t = C_\mu \rho \frac{k^2}{\varepsilon} f_\mu \quad (6)$$

where ε – dissipation rate of turbulent kinetic energy, f_μ – wall-adjacent function, equal to $f_\mu = 1 - \exp(-0.0115y_*)$.

Differential equations of turbulent kinetic energy and its dissipation rate are as follows:

$$\rho u \frac{\partial k}{\partial z} + \rho v \frac{\partial k}{\partial r} = \frac{\partial}{\partial z} \left(\mu_\varepsilon \frac{\partial k}{\partial z} \right) + \frac{1}{r} \frac{\partial}{\partial r} \left(r \mu_\varepsilon \frac{\partial k}{\partial r} \right) + P_k - \rho \varepsilon - \frac{2\mu k}{y^2} \quad (7)$$

$$\begin{aligned} \rho u \frac{\partial \varepsilon}{\partial z} + \rho v \frac{\partial \varepsilon}{\partial r} &= \frac{\partial}{\partial z} \left(\left(\mu + \frac{\mu_t}{\sigma_\varepsilon} \right) \frac{\partial \varepsilon}{\partial z} \right) + \frac{1}{r} \frac{\partial}{\partial r} \left(r \left(\mu + \frac{\mu_t}{\sigma_\varepsilon} \right) \frac{\partial \varepsilon}{\partial r} \right) + \\ &+ C_1 \frac{\varepsilon}{k} P_k - C_2 \frac{\rho \varepsilon^2}{k} f_e - \frac{2\mu \varepsilon}{y^2} g_e \end{aligned} \quad (8)$$

where f_e, g_e – wall-adjacent function (Chien *et al.*, 1982) equal to

$$f_e = 1 - 0.22 \exp \left(-\frac{Re_t^2}{36} \right), \quad g_e = \exp(-0.5y_*) \quad (9)$$

Constants $(k - \varepsilon)$ – models equal to $C_1 = 1.35, C_2 = 1.8, C_\mu = 0.09, \sigma_\varepsilon = 1.3$.

The physical Prandtl number (Pr) is determined by the initial temperature of the liquid T_o and is taken as equal to $Pr = 0.9$. The turbulent analog of the Prandtl number Pr_t – according to (Chen *et al.*, 1988, Chien *et al.*, 1982) can also be taken equal to $Pr_t = 0.9$.

For more convenience the heat transfer equation can be written in relation to the excess-temperature $\theta = (T - T_w)/(T_o - T_w)$, where T_w – oil temperature in the bottom of the pit.

The system of equations (1)–(9) is reduced to the dimensionless variables. Axes z and r are divided by the radius of the jet entrance section, velocity components u and v – by the maximum velocity of the jet at the entrance, pressure p – by the maximum value of the dynamic pressure of the jet, temperature T – by T_o ; density, dynamic viscosity, thermal conductivity and heat capacity coefficients – by the values of these quantities at temperature T_o .

The boundary conditions of the task are as follows:

$$z = 0: \quad 0 \leq r \leq 1; \quad u = f(r); \quad v = 0; \quad k = k(r); \quad \theta = g(r); \quad \varepsilon = \varepsilon(r) \quad (10)$$

$$z = 0: \quad 1 < r \leq R_w; \quad \tau = u = k = \varepsilon = 0; \quad -\frac{\partial \theta}{\partial z} = Bio_f \theta \quad (11)$$

$$\begin{aligned}
z = L: \quad 0 < r \leq R_w; \quad u = v = k = \varepsilon = 0; \quad -\frac{\partial \theta}{\partial z} = Bio\theta \\
r = 0: \quad 0 \leq z \leq L; \quad \frac{\partial u}{\partial r} = v = \frac{\partial \theta}{\partial r} = \frac{\partial k}{\partial r} = \frac{\partial \varepsilon}{\partial r} = 0 \\
r = R_w; \quad 0 \leq z \leq L; \quad u = v = k = \varepsilon = 0; \quad -\frac{\partial \theta}{\partial r} = Bio\theta
\end{aligned} \tag{12}$$

The boundary conditions at the upper boundary ($z = 0$) for axial velocity component, turbulent kinetic energy and its dissipation rate, excess temperature in jet entrance section (10) correspond to developed motion of a round turbulent jet flow and beyond the flow inlet area (11) the conditions on free surface (equal to zero in shearing stress (Batchelor *et al.*, 1973) are effective. At the lower solid surface ($z = L$) adhesion and heat exchange in a frontal interaction of the jet flow with an obstacle are effective, on the left boundary ($r = 0$) – the conditions of symmetry of the flow motion, and on the right ($r = R_w$) – adhesion and the heat exchange with the surrounding soil are effective.

The system of equations (1)–(9) with boundary conditions (10)–(12) is solved numerically in variables of stream function and vortex strength.

Stream function ψ is introduced to satisfy motion continuity equation by the following equations:

$$\rho ru = \frac{\partial \psi}{\partial r}, \quad \rho rv = -\frac{\partial \psi}{\partial z} \tag{13}$$

and vortex strength – by a standard expression:

$$\omega = \frac{\partial v}{\partial z} - \frac{\partial u}{\partial r} \tag{14}$$

Substituting (13) into (14) we get an equation for defining the stream function:

$$\frac{\partial^2(\psi/\rho r)}{\partial^2 r} + \frac{\partial^2(\psi/\rho r)}{\partial^2 z} + \omega = 0 \tag{15}$$

and from the system of motion equations excluding the pressure – we get an equation for the vortex strength (Gosman *et al.*, 1969, Roach *et al.*, 1979):

$$r^2 \left[\frac{\partial}{\partial z} \left(\frac{\omega \partial \psi}{r \partial r} \right) - \frac{\partial}{\partial r} \left(\frac{\omega \partial \psi}{r \partial z} \right) \right] = \frac{\partial}{\partial z} \left[r^3 \frac{\partial}{\partial z} \left(\mu_\varepsilon \frac{\omega}{r} \right) \right] + \frac{\partial}{\partial r} \left[r^3 \frac{\partial}{\partial r} \left(\mu_\varepsilon \frac{\omega}{r} \right) \right] + S_\omega \tag{16}$$

where S_ω – source element is determined, as in Gosman *et al.*, 1969.

The boundary conditions for equations (15), (16) are easily obtained from (10)–(12):

$$z=0: \quad 0 \leq r \leq 1; \quad \omega = \omega_o(r); \quad \psi = \psi_o(r); \quad \theta = \theta_o(r); \quad k = k_o(r); \quad \varepsilon = \varepsilon(r)$$

$$z=0: \quad 1 < r \leq R_w; \quad \omega = \frac{\partial \psi}{\partial r} = k = \varepsilon = 0; \quad -\frac{\partial \theta}{\partial z} = Bio_f \theta \quad (17)$$

$$z=L: 0 < r \leq R_w; \quad \psi = k = \varepsilon = 0; \quad -\frac{\partial \theta}{\partial z} = Bio \theta; \quad \omega_w = -\frac{2^*(\psi_p - \psi_w)}{r_w h_p^2 \rho_w}$$

$$r=0: \quad 0 \leq z \leq L; \quad \omega = \psi = \frac{\partial \theta}{\partial r} = \frac{\partial k}{\partial r} = \frac{\partial \varepsilon}{\partial r} = 0 \quad (18)$$

$$r=R_w: \quad 0 \leq z \leq L; \quad \psi = k = \varepsilon = 0; \quad -\frac{\partial \theta}{\partial r} = Bio \theta; \quad \omega_w = -\frac{2^*(\psi_p - \psi_w)}{R_w h_p^2 \rho_w}$$

Boundary conditions on solid surfaces for vortex strength are defined using Thomas equation (Gosman *et al.*, 1969, Roach *et al.*, 1979).

For the finite-difference analogues of differential equations the control volume approach in difference grid with irregular pitch is applied. The grid step in direction of OZ axis is clumped close to entrance region and tank bottom. Grid size on OR direction is increase close to the boundary of mixing zone of jet and surrounding fluid and close to the solid sidewall. Grid size of 191×161 was used in calculations. Calculation time of one operation in personal computers is 600 sec.

The vortex strength, heat conduction, turbulent kinetic energy and its dissipation rate equations were approximated by a hybrid scheme (Gosman *et al.*, 1969, Roach *et al.*, 1979, Shi *et al.*, 1988). Difference analogs of vortex strength, heat transfer, turbulent kinetic energy and its dissipation rate equations calculated by Gauss-Seidel method, and stream function by over-relaxation method (Gosman *et al.*, 1969, Roach *et al.*, 1979).

Mathematical model and numerical method was validated by solving task of flat turbulent jet of air that running over heated flat sidewall. Estimated data for evaluation of local Stanton number, which expresses the heat transfer between the wall and streamline flow were compared with calculations of Spalding (Gosman *et al.*, 1969) and experimental data of Gardon and Akifrat (Gardon *et al.*, 1965) (Fig. 2). The comparison results in developed turbulence ($Re = 11\,000, 22\,000$) show that the calculated results match the experimental data (Gardon *et al.*, 1965). For $Re = 5500$, some deviation from experiment has been occurred, though a qualitative matching of the local Stanton number is quite good (Fig. 2). It should be noted that such fundamental laws of turbulent jet flow, such as: 1) linear law of

the jet boundary development, and 2) Reynolds analogy between dynamic and heat transfer characteristics of averaged and a pulsating flow is well satisfied in the calculation.

Thus, validation of model and numerical method provides a reasonable basis for the confidence of results.

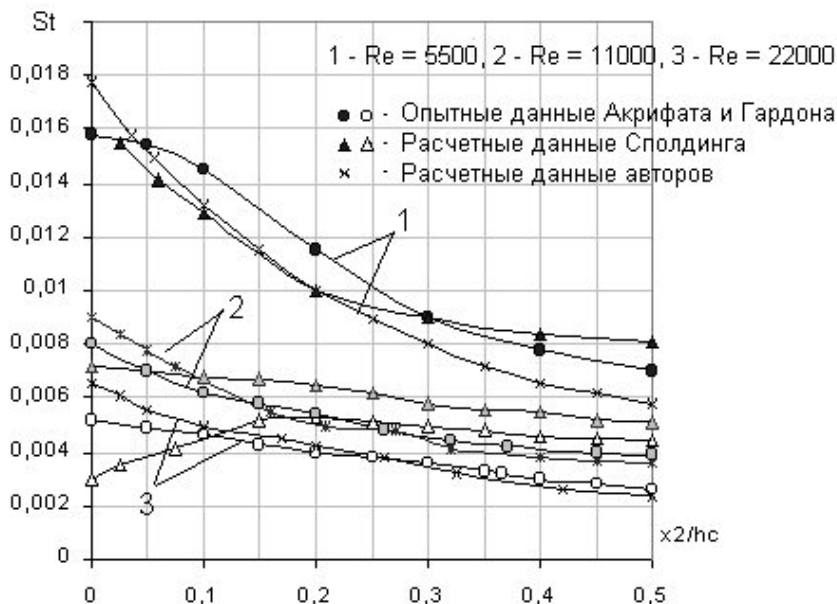


Fig. 2. Results of validation model and calculation method

2. CALCULATION DATA

The main operating parameters in the calculation-theoretical study are Reynolds number Re (calculated by average velocity and diameter of jet in entrance section), the Bio number (expressing the fluid heat transfer at the bottom and side wall of tank), the Bio_f number (expressing the heat transfer fluid on the exposed surface); hc/Rc , Rw/Rc ratios, where hc – the distance between the nozzle and bottom of tank, and Rc , Rw – nozzle and tank radiiuses, respectively, Pr laminar and Prt turbulent Prandtl numbers.

Figure 5.3 shows the isoline of over temperature θ , turbulent viscosity μ_e , stream function ψ , vortex strength ω , velocity \vec{V} , turbulent kinetic energy k and dissipation rate of turbulent kinetic energy ε at $Re = 11\ 000$, $Bio = 1$, $Bio_f = 5$, $Pr_i = 0,9$, $hc/Rc = 29$ and $Rw/Rc = 6$. Heat transfer at free surface is much higher than on the walls of tank, so in calculations Bio_f taken greater than Bio .

Flow structure consists of three parts: 1) Fluid flow part, directed to the bottom of oil pit, and 2) region of reverse flow with circulation region of a toroidal vortex, and 3) boundary layer flow on the side walls of tank, directed toward the free surface of the tank.

The law of non-isothermal turbulent jet in pit oil may proposed by distributions of stream function ψ , velocity vector \vec{V} , over temperature θ . On the contrary the boundary changes of well known linear law of turbulent jet in submerged space (Abramovich *et al.*, 1960), investigated boundary of jet flow strongly curved and expanded (Fig. 3a). This behavior of the jet boundary in the tank can be explain the strong dependence of oil viscosity on temperature. Pit oil at environmental temperature ($T_W = 303\text{K}$) and is involved in jet motion due to friction forces. Hot jet ($T_o = 373\text{K}$) heats pit oil through the convective mixing, molar and molecular heat conduction and dissipation of mechanical energy into heat. Value of the over-temperature is maximum on the axis and decreases to the borders of jet, and oil viscosity vice versa, takes its minimum value at jet axis and increases outside of jet flow. Initially, the calculated ratio of maximum and minimum values of viscosity in range of jet section is equal to $\mu_{\max}/\mu_{\min} = 11.8$. High oil viscosity and its dependence on temperature of a rapid expansion of the jet boundary resulted. In addition, system of equations includes turbulent viscosity, which characterizes influence of turbulent stress on the flow structure. Isolines pattern show the distribution of turbulent viscosity in computational domain (Fig. 3b). It is easy to see that there is a maximum value field of μ_t , covering, the jet interaction zone with reverse flow and jet deceleration zone. Concentrating of turbulence energy in these areas is resulted the large values of μ_t and hence turbulent stresses.

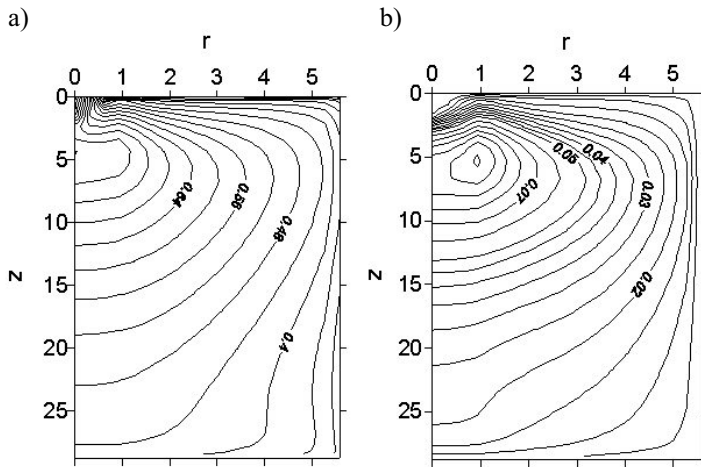


Fig. 3. Distribution of isotherm curves (a) and isolines of turbulent viscosity (b)

Toroidal vortex flow structure has significant influence for transfer processes (Fig. 4a). Closed contours of the stream function ψ are characterized involvement of pit oil fluid mass in vortex motion. In the stagnation zone fluid rotates slightly, transferring the heat of hot jet into the cold part and warming pit oil. The vortex strength ω isolines in the flow jet part and on the side wall are noticeable, and at remaining part their values negligible (Fig. 4b).

Flow pattern in more detail reveals the isolines of the velocity vector \vec{V} (Fig. 5).

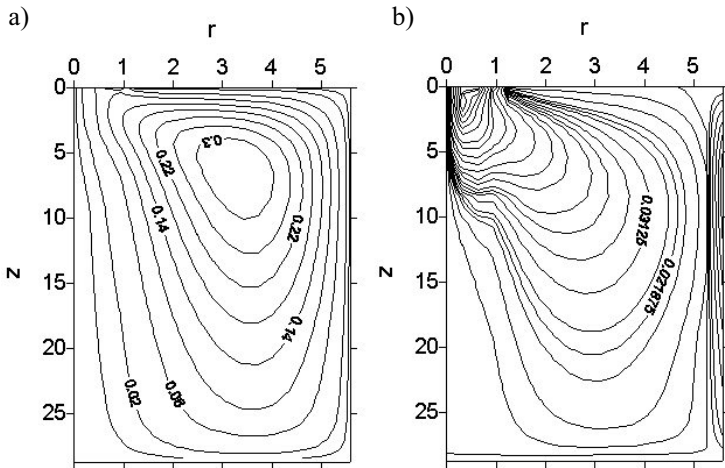


Fig. 4. Isolines of stream function (a) and vortex strength (b)

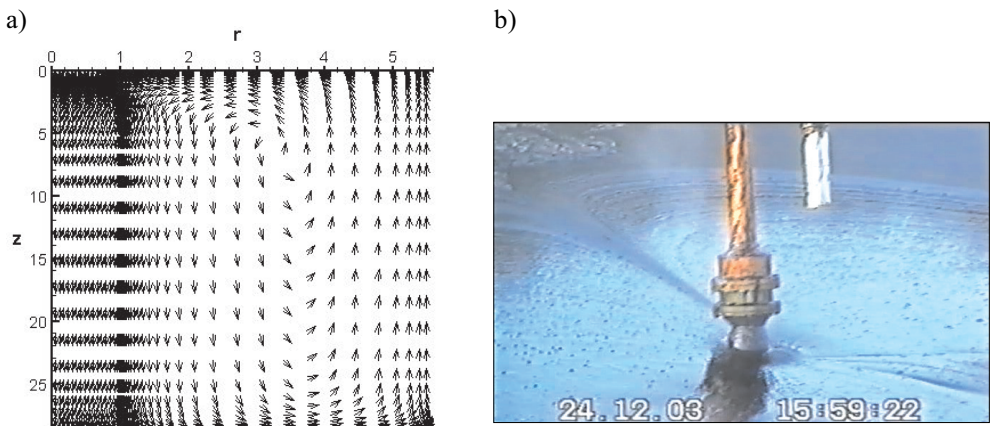


Fig. 5. Isolines of velocity vector: calculated data (a) and photo of pit oil jet development (b)

Velocity vector in jet part is directed downward, close to its borders involvement of fluids in motion is observed. The jet flowed to the bottom of tank, which leads to change in the direction of velocity vector on 90 degrees and wraps around the pit bottom. In vortex motion zone fluid reverse flow is occurred. Velocity vector along the side wall is directed vertically upwards, and changes direction on 90 degrees close to free surface, which corresponds to observed pattern of the pit oil liquefying phenomenon in the industrial test (Fig. 5b).

Thus, the overall flow pattern can be represented as jet involvement in recirculation flow in pit oil. Convection process of heating pit oil is dominated in calculations and tests. Hot liquid intaking and mixing it with cold pit oil is occurred in vortex zone. Heat dissipation of kinetic energy is diffused through convection and molar transfer. Therefore, local heating zone due to the heat dissipation does not occur.

The distribution of turbulent kinetic energy k isolines has region of maximum turbulence energy (Fig. 6a). This area is intense of turbulence energy concentration due to ejection of fluid jet from pit oil. A flow change of turbulent kinetic energy in remaining part is negligible.

The maximum value in dissipation rate of turbulent kinetic energy isolines (Fig. 6b) is achieved in zone involving a jet of pit oil, and in the peripheral part their values are low. Calculated results of turbulent flow characteristics show that the molar transfer plays an important role in jet part and vortex zone. Convection and molecular mechanism transfer of turbulent kinetic energy dissipation rate is dominated in remaining part of flow.

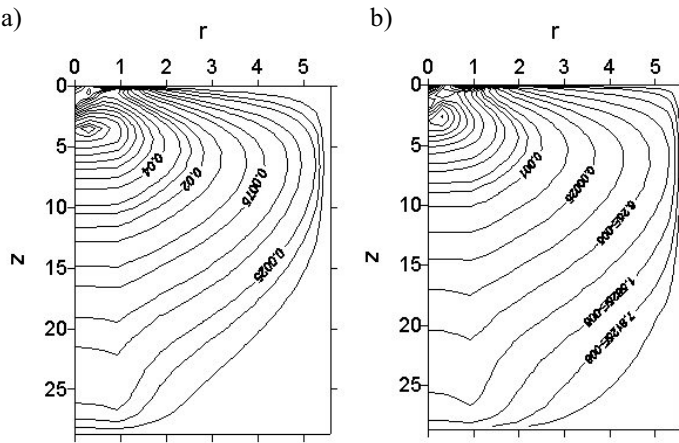


Fig. 6. Isolines of turbulent kinetic energy (a) and turbulent kinetic energy dissipation rate (b)

The turbulent heat transfer λ_t , identified using the turbulence model ($k - \varepsilon$), which express the molar heat transfer is fluctuating as μ_t . These data confirm the similarity between heat transfer process and momentum in turbulent flow.

3. CONCLUSIONS

According to results of study following conclusion can be drawn:

1. A mathematical model of turbulent non-isothermal jet flow development in pit oil and numerical computation of mathematical model were developed.
2. Mathematical model and numerical computation validation show a good agreement both with calculated results and experiments;
3. The low Reynolds two equation ($k - \varepsilon$) – turbulence model is qualitatively good detected the basic objective law of momentum and heat transfer in the development of non-isothermal jet flow in pit oil;

4. The flow structure consists of three parts are shown: 1) jet flow part 2) reverse flow in the toroidal vortex, 3) boundary layer flow of a viscous fluid close the side wall;
5. Calculated results are in qualitative agreement with the observed process and show that turbulent (molar) transfer plays an important role in the jet zone and eddy zone of reverse flow. In remaining part convection and molecular mechanism of momentum and heat transfer is dominated;
6. Developed mathematical model and numerical computation give opportunity to study the process of heating pit oil using hot fluid jet. In technical aspect it affords to identify the mass of pit oil heated to proper temperature for thermo-mechanical technology of gathering spilled oil.

REFERENCES

- Yershin S.A., Zhabasbayev U.A., Aisayev S.U., Utegaliyev S.A., Khairov G.B.: Patent #10116. Pit oil gathering and equipment, 2002.
- Abramovich G.N.: *Theory of turbulent jet*. Phizmatgiz, Moscow 1960, vol. 577.
- Shlikhting G.: *Boundary layer theory*. Nauka, Moscow 1974, vol. 707.
- Loytsanski L.G.: *Fluid Mechanics*. Nauka, Moscow 1987, vol. 840.
- Sebesi T., Bredshou P.: *Convection heat transfer. Physical basis and computation aspects*. 1987, vol. 592.
- Moulden M.: Mir, Moscow 1980, vol. 377.
- Koolman V.: *Calculation method of turbulent flow*. Mir, Moscow 1984, vol. 464.
- Shets J.: *Turbulent flow. The processes of injection and mixing*. Mir, Moscow 1984, vol. 247.
- Chen H.C., Patel V.C.: *Near-wall turbulence models for complex flows including separation*. AIAA J. V. 26., 1988, pp. 641–648.
- Menter F.R.: *Two-Equation Eddy-Viscosity Turbulence Models for Engineering Applications*. AIAA J. V. 32., 1993, pp. 1598–1604.
- Craft T.J., Gerasimov A.V., Iacovides H., Kidger J.W., Launder B.E.: *The Negatively Buoyant Turbulent wall Jet: Performance of Alternative Options in RANS Modelling*. Proc. 4th Int. Symp. On Turbulence, Heat and Mass Transfer, Antaly, Turkey, 2003, pp. 813–820.
- Chien K.Y.: *Predictions of channel and boundary layer flows with low Reynolds-number two-equation model of turbulence*. AIAA J., V. 20, No. 1, 1982, pp. 33–38.
- He S., Xu Z., Jackson J.D.: *An experimental investigation of buoyancy – opposed wall jet flow*. Int. J. Heat and Fluid Flow., V. 23. 2002, pp. 487–496.
- Batchelor J.: *Introduction to fluid dynamics*. M. Mir, 1973, vol. 757

- Gosman A.D., Pun W.M., Runchal A.K., Spalding D.B., Wolfshtein M.: *Heat and Mass Transfer in Recirculating Flows*. London and New York, 1969, 309 p.
- Roach P.: *Computational Fluid Mechanics*. Mir, Moscow 1979, vol. 487.
- Shi D.: *Numerical methods in heat transfer*. Mir, Miscoow 1988, vol. 544.
- Gardon R., Akifrat J.C.: *The role of turbulence in determining the heat transfer characteristics of impinging jets*. Int. J. Heat Mass Transfer., V. 8., 1965, pp. 1261–1272.